Eur Biophys J (2001) 30: 500–514
DOI 10.1007/s002490100175

ARTICLE

J. Šimurda · M. Šimurdová · M. Pásek · P. Bravený

Quantitative analysis of cardiac electrical restitution

Received: 27 March 2001 / Revised version: 14 June 2001 / Accepted: 14 June 2001 / Published online: 6 September 2001

Abstract Electrical restitution (ER) of cardiac cells is an aggregate of events that rhythmically restore the initial conditions of electric signal (action potential) generation. Its analysis represents an important insight into cardiac arrhythmogenesis. The aim of this work is to theoretically substantiate and verify a novel approach allowing for the quantification of the individual ionic current components of ER. A method of analysis of the primary, initial conditions-setting restitution processes (apart from the secondary, test pulse-affected ones) is proposed. Both processes are described as sums of their measurable constituents. It is demonstrated that the optimum parameter of ER is the electric charge that is transferred through ionic channels and carriers during the test impulse. The theory was tested by using voltage-clamped canine ventricular preparations and by computer simulations. The experimental ER curve of canine ventricular muscle was constructed using action potential (AP) plateau voltage and half-repolarization time as parameters. At 30 °C and 0.5 Hz stimulation, the ER curve peaked, on average, after 400 ms with a 10% overshoot. Of this plateau elevation, 50% was due to 4-aminopyridine-sensitive transient outward current and 44% was due to verapamil-sensitive current. The delayed outward current antagonized the overshoot by about 6%. It was found that the initial conditions (i.e. the primary restitution processes) tend to strongly alter the plateau voltage of the premature AP. However, the final deviation is by about one order less. It is concluded that the voltage-dependent secondary processes counteract the effect of the primary processes, thereby suggesting strong negative feedback control of natural APs.

J. Šimurda (✉) · M. Šimurdová · M. Pásek · P. Bravený
Department of Physiology, Faculty of Medicine,
Masaryk University, 662 43 Brno, Czech Republic
E-mail: simurda@med.muni.cz
Fax: +42-5-42126561

Keywords Electrical restitution · Heart cells · Membrane currents · Action potentials · Quantitative analysis

Abbreviations and symbols AP: action potential · APV, APD: voltage and duration of AP (the subscripts in APV_{Td}, APD_{50}, etc., specify the reading) · *4-AP*: 4-aminopyridine · *ER*: electrical restitution · $[Ca^{2+}]_i$: intracellular Ca^{2+} concentration · $[K^+]_e$: extracellular K^+ concentration · C: linear membrane capacity · I_{bg}: time-independent background current · I_C: membrane capacity current · I_{Ca}: calcium inward current · I_i: total ionic membrane current · I_K: delayed outward current · I_{Kr}, I_{Ks}: rapid and slow components of I_K · I_m: total membrane current · I_{Na}: sodium inward current · I_{NaCa}: Na/Ca exchange current · I_{si}: slow inward current · I_{to}: potassium transient outward current · I_{to1}: 4-AP sensitive component of $I_{to;}$ · I_{to2}: component of I_{to} activated by Ca^{2+} · I_{vs}: verapamil-sensitive current · Q_m, Q_i: charge represented by time integrals of I_m and I_i with negative sign · $Q^p_K, Q^p_{vs}, ..., Q^p_j$: charge transferred by I_K, I_{vs}, ..., I_j in response to rectangular test pulse · $\Delta Q^p(T)$, $\Delta Q^s(T)$,...: charge represented ER curves (primary and secondary) $\Delta Q^p_{Ca}, \Delta Q^p_K, \cdots$: ionic components of $\Delta Q^p(T)$ · ΔQ^s_{Ca}, $\Delta Q^s_K, \cdots$: ionic components of $\Delta Q^s(T)$ · T: variable test interval · T_d: instant of reading APV and upper limit of current integration · T_o: period of regular stimulation · U: membrane voltage

Introduction

The well-known plasticity of the cardiac action potential (AP) configuration is an inherent feature of the physiological control of intracellular calcium and thereby of a number of vital processes, including contraction. Moreover, the abnormalities of AP duration and refractoriness represent a significant arrhythmogenic terrain (Morgan et al. 1992a; Watanabe et al. 1995; Koller et al. 1998; Wu et al. 1999; for review see Janse and Wit 1989). The prominent

rate- (or interval-) dependent variations of AP configuration reflect the intricately orchestrated recovery of the ionic transport mechanisms from the preceding excitation, known as electrical restitution (ER). Indeed, the duration and plateau height of the premature AP have become the standard measures of the dynamics of membrane processes (Bass 1975; Iinuma and Kato 1979; Elharrar and Surawicz 1983; Robinson et al. 1987; Qi et al. 1997).

ER has been suggested to mirror the recovery of different time-dependent current components with different kinetics: depolarizing inward calcium current I_{Ca} (Tseng 1988; Peineau et al. 1992), two types of repolarizing potassium transient outward current I_{to} (Kawano and Hiraoka 1991), delayed outward potassium current I_K (Zeng et al. 1995), and $[Ca^{2+}]_i$-dependent current components including Na/Ca exchange current I_{NaCa} (Kobayashi et al. 1992; Janvier et al. 1997; Szigligeti et al. 1998). Thus, ER may be defined as the processes of recovery from preceding excitation which determine the initial conditions of the next excitation. These processes namely contain the recovery from inactivation or deactivation of ionic channels and the equilibration of ionic concentrations in the relevant compartments. Though transient changes of most of the quantities involved are not directly measurable, they determine the initial conditions of measurable ionic currents developed in response to depolarizing test pulses.

The usual choice of premature AP as a test pulse with its duration and plateau height as the parameters characterizing ER is natural and fully justified from the practical point of view. However, it becomes problematic if ER is analysed in terms of the underlying ionic currents, i.e. if the current components responsible for ER are to be identified and quantified. The shortcomings result from the fact that the above-mentioned ER parameters cannot be read at the starting point of the test AP, but only during its later course. Therefore, they are not only determined by the currents recovering between the excitations, but also by their modulation during the running test excitation itself. This drawback is particularly critical when using specific inhibitors to identify the current components. The second drawback of the methods to this point is that the usual measures of current components are non-additive; hence the analysis cannot be strictly quantitative.

This paper describes a quantitative approach to the analysis of ER in terms of the underlying ionic current components. The proposed method eliminates the ambiguity in the evaluation of the components primarily responsible for ER: the real restitution processes that determine the initial conditions of the test AP are explored separately from the processes occurring during the test AP up to the time of parameter reading. Furthermore, we demonstrate that the most significant quantity for evaluating the role of individual restituting current components is the electric charge transferred across the membrane.

Methods

Preparation and experimental arrangement

The reported novel approach to electrical restitution analysis was derived from experimental data obtained in the long running of our research of ER. All the details of the experimental arrangement, including the substantiation of the technique, have been described elsewhere (Šimurda et al. 1976, 1992). In brief, thin trabeculae (less than 0.7 mm in diameter) without branches and residual Purkyne fibres were excised from the right ventricles of adult mongrel dogs, which were under deep urethane anaesthesia. Membrane voltage was measured by conventional 3 M KCl-filled glass microelectrodes (10–30 MΩ) connected to a high input-impedance amplification system. Membrane currents were recorded employing the voltage clamp method in a single sucrose gap arrangement. Initially, all three compartments of the tissue chamber were perfused with a Tyrode solution gassed with a mixture of 95% O_2 + 5% CO_2. After 40 min of equilibration of the stimulated muscle, the perfusion of two compartments was changed: in the rear compartment by KCl Tyrode; in the middle one by sucrose. The membrane currents were then recorded using the voltage-clamp regimen. The temperature of the solutions was maintained at 30 ± 0.2 °C. The experimental data used in the verification of the proposed method were derived from nine experiments.

Solutions and drugs

The modified Tyrode solution contained the following (in mM): 149.9 Na; 5.4 K; 1.8 Ca; 0.5 Mg; 145.0 Cl; 11.9 HCO_3; 0.32 H_2PO_4; 5.0 glucose; pH 7.2–7.4. The isotonic sucrose solution contained 5 mM glucose and 0.1 mM $CaCl_2$. In the KCl Tyrode solution, 120 mM Na was substituted by K. The sucrose solution was gassed with 100% O_2. The blocking agents verapamil (10 μM, Isoptin Lek) and 4-aminopyridine (4-AP) (1–2 mM, Sigma) were added to the Tyrode solution from concentrated stock solutions. In order to abolish the possible secondary effect of 4-AP on membrane currents due to noradrenaline release (Yanagisawa and Taira 1979), the beta blocking agent pindolol (30 nM, Visken, Sandoz) was applied 1 h before 4-AP into the perfusion fluid in four preparations.

AP and membrane current recording

The preparations were stimulated at a basal rate of 0.5 Hz by rectangular pulses (1 ms duration, twice the threshold intensity). The following AP parameters were measured: voltage achieved after a constant interval of $T_d = 100$ ms from the stimulating pulse (APV_{100}) and duration at a level of 50% repolarization (APD_{50}). Restitution of AP parameters was determined from the responses to single test stimuli delivered after every eighth beat at the basal rate. The test interval (T in Fig. 1b) was measured from the stimulating pulse of the last steady-state AP. It was progressively increased from 0.3 to 2 s.

The voltage-clamp stimulation protocol used for the construction of the ER curve in terms of electric charge (charge-ER curve) consisted of a sequence of eight rectangular impulses (80 mV from resting potential for 300 ms) at a rate of 0.5 Hz followed by a test pulse of identical voltage and duration, but of variable prematurity. The membrane currents elicited by the test pulse were sampled at 0.5 ms time intervals and stored for further processing.

The transferred charge was calculated as the sum of current samples multiplied by the sampling interval. The integration was carried out between 10 and 200 ms from the onset of the clamp pulse. The lower limit of integration (10 ms) allows the complete fading out of the fast depolarization current I_{Na}; the upper limit (200 ms) corresponds to the average APD_{50}. In five earlier oscillographic records (Mingograph 34 Elema, bandwidth 0–750 Hz, ±10%) the area under the recorded currents was enlarged, scanned, and evaluated by a specially designed computer program. For

the sake of comparison between the charge-ER curve and conventional AP restitution, it was expressed in voltage units as the ratio of charge to linear membrane capacity (C). Estimated from the exponential responses of membrane current to negative 10 mV voltage clamp pulses from the resting potential, C ranged between 1.05 and 2.1 μF.

Computer model

The proposed method of ER analysis was verified on a quantitative model (Nordin 1993) modified by the incorporation of the 4-AP-sensitive transient inward current I_{to1}. On the basis of experiments with canine ventricular fibres (Šimurda et al. 1988; Tseng and Hoffman 1989), we described I_{to1} as follows:

$$I_{to1} = \overline{g_{to1}} y_1 (U - U_K) \tag{1}$$

where U is the membrane voltage, U_K is the Nernst reversal voltage of K^+, $\overline{g_{to1}} = 0.05$ μS, and y_1 results from the solution of a set of four differential equations:

$$\begin{aligned}
\frac{dy_1}{dt} &= -(\alpha_r + \beta_q) y_1 + \beta_r y_2 + \alpha_q y_4 \\
\frac{dy_2}{dt} &= \alpha_r y_1 - (\beta_q + \beta_r) y_2 + \alpha_q y_3 \\
\frac{dy_3}{dt} &= \beta_q y_2 - (\alpha_q + 0.05\beta_r) y_3 + 0.05\alpha_r y_4 \\
\frac{dy_4}{dt} &= \beta_q y_1 + 0.05\beta_r y_3 - (0.05\alpha_r + \alpha_q) y_4
\end{aligned} \tag{2}$$

where:

$$\begin{aligned}
\alpha_q &= \frac{0.395}{1 + e^{-0.081(U+0.9)}} \\
\beta_q &= \frac{0.356}{1 + e^{0.0463(U+12.4)}} \\
\alpha_r &= \frac{0.076\, e^{-\frac{U+80}{26.6}}}{1 + e^{0.4(U+48)}} \\
\beta_r &= \frac{0.075 e^{\frac{U-50}{95.9}}}{1 + e^{-0.4(U+49.4)}}
\end{aligned} \tag{3}$$

The calculations presented in the Results section respect, with only minor exceptions, Nordin's original numerical values of constants that describe the individual current components. For the sake of simplicity, the calcium-activated currents (K^+ current and the non-specific cation current) were treated as a total and denoted as I_{to2}. The constants pertaining to I_{Ca} and I_{NaCa} were set respectively at $\alpha_{f_2} = 25\ s^{-1}$ and $k_{Na/Ca} = 0.0012$. Also the rate constants of I_{Na} had to be modified to achieve full spike. Nevertheless, the influence of I_{Na} on the ER course was negligible.

The resultant total set of non-linear differential equations was solved using the Runge Kutta fourth-order adaptive step algorithm in Merson's modification. To ensure numerical accuracy, the maximum interval of calculation was set to 0.1 ms and the maximum relative error for all variables in each iteration was 10^{-8}.

Theory

The present quantitative analysis is based on the assumption that the parameters of electrical restitution meet the following criteria:

1. they separately describe the primary restitution processes determining the initial conditions of premature AP and the secondary ones resulting from the processes occurring during the variable test AP;
2. they are expressed as sums of the contributing current components;
3. the contributions of the individual components are measurable quantities.

Assuming that, under the given experimental conditions, the membrane voltage U does not depend on spatial coordinates and is merely a function of time, the membrane current I_m from an external source may be expressed as a sum of the capacity current $I_C = C(dU/dt)$, the ionic membrane current I_i, and the transient gating currents I_g:

$$I_m = C\frac{dU}{dt} + I_i + I_g \tag{4}$$

Though the gating currents appear to participate in the constitution of the AP configuration, their effect may be estimated by about two orders less in comparison with the effect of corresponding ionic current components (see Discussion). For the sake of simplicity, they are omitted in the following text. However, they may be reintroduced if necessary, following the same principles as described for the ionic currents below.

The current I_i is the sum of its n components $I_{i,j}$, which represent the currents through the membrane channels and by the carriers:

$$I_i = \sum_{j=1}^{n} I_{i,j} \tag{5}$$

The integration of Eq. (4) at any time interval $< T, T + T_d >$ gives the relation between corresponding membrane voltages $U(T + T_d)$ and $U(T)$ (Fig. 1a), both in current-clamp and in voltage-clamp modes:

$$U(T + T_d) = U(T) + \frac{1}{C}\int_{T}^{T+T_d} (I_m - I_i)\,dt \tag{6}$$

Denoting

$$\begin{aligned}
Q_m(T, T_d) &= -\int_{T}^{T+T_d} I_m(t)\,dt, \\
Q_i(T, T_d) &= -\int_{T}^{T+T_d} I_i(t)\,dt
\end{aligned} \tag{7}$$

then Eq. (6) can be written in the form:

$$U(T + T_d) = U(T) + \frac{Q_i(T, T_d)}{C} - \frac{Q_m(T, T_d)}{C} \tag{8}$$

where $Q_i(T, T_d)$ represents the total electric charge transferred by ionic currents across the membrane during interval $< T, T + T_d >$. It may be written as a sum of the charges related to individual current components:

$$Q_i(T, T_d) = -\sum_{j=1}^{n} \int_{T}^{T+T_d} I_{i,j}(t)\,dt = \sum_{j=1}^{n} Q_{i,j}(T, T_d) \tag{9}$$

Now $Q_m(T, T_d)$ is a measurable quantity. It represents an integral of the recorded current, i.e. the total charge supplied by the source of the membrane current under

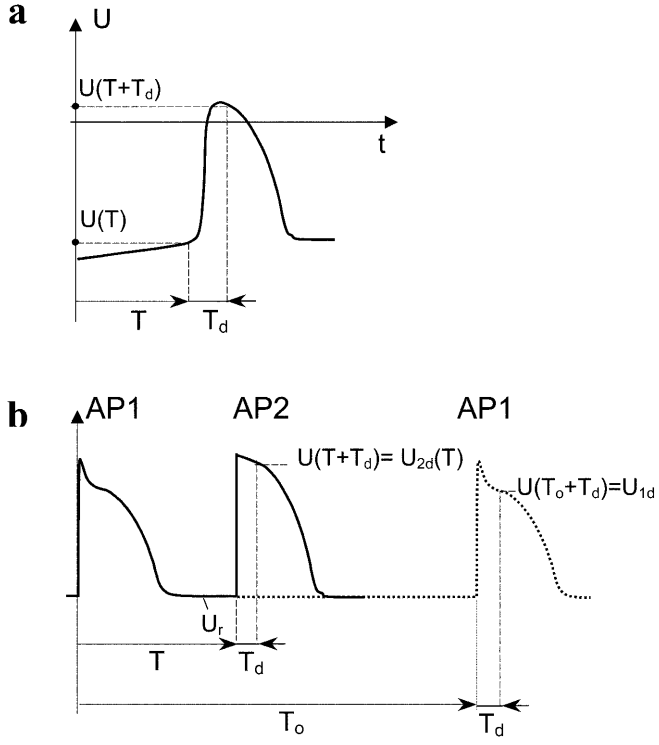

Fig. 1a, b Graphic representation of the quantities employed in the theoretical analysis of electrical restitution

voltage-clamp or current-clamp conditions. If the free-running APs are recorded under current-clamp conditions then, as a rule, the charge supplied during a short supra-threshold stimulation impulse remains constant.

Definition of the parameters ΔQ^{p} and ΔQ^{s}

In the following considerations, let us denote AP1 to be the course of the steady-state AP recorded at regular driving with a period of T_{o}, and AP2 to be the course of AP recorded after a single altered interval T (Fig. 1b). The intervals are measured between the onsets of the stimulating pulses. The membrane voltage $U(T)$ then equals the resting membrane voltage U_{r}. The electrical restitution can be characterized by the membrane voltage $U(T+T_{\mathrm{d}})$ (T_{d} is a selected constant interval). In accordance with the numbering of regular and premature AP, let us denote $U(T_{\mathrm{o}}+T_{\mathrm{d}})=U_{1\mathrm{d}}$ and $U(T+T_{\mathrm{d}})=U_{2\mathrm{d}}(T)$. The waveforms of AP recorded in current-clamp mode can be stored in memory and then imposed in voltage-clamp mode after varied intervals. Using the above notation, Eq. (8) takes the form:

$$\begin{aligned} U_{1\mathrm{d}} &= U_{\mathrm{r}} + \frac{Q_{\mathrm{i},1}(T)}{C} - \frac{Q_{\mathrm{m},1}(T)}{C} \\ U_{2\mathrm{d}}(T) &= U_{\mathrm{r}} + \frac{Q_{\mathrm{i},2}(T)}{C} - \frac{Q_{\mathrm{m},2}(T)}{C} \end{aligned} \tag{10}$$

where the subscripts 1 and 2 refer to AP1 and AP2. As T_{d} is a constant parameter, the functional dependence of charges on T_{d} is omitted. (For example, $Q_{\mathrm{m},1}(T) = -\int_{T}^{T+T\mathrm{d}} I_{\mathrm{m}}(t)\mathrm{d}t$ denotes a charge obtained by the integration of the current recorded in response to the stored AP1 waveform which is voltage clamped after a premature test interval of T.) Equations (10) hold for any T, particularly for $T=T_{\mathrm{o}}$. Consequently (taking into account that $U_{1\mathrm{d}}$ is a constant):

$$Q_{\mathrm{i},1}(T) - Q_{\mathrm{i},1}(T_{\mathrm{o}}) = Q_{\mathrm{m},1}(T) - Q_{\mathrm{m},1}(T_{\mathrm{o}}) \tag{11}$$

Let Q_{st} be a constant charge delivered by a short supra-threshold current impulse from an external source in current clamp mode. Evidently:

$$Q_{\mathrm{m},1}(T_{\mathrm{o}}) = Q_{\mathrm{m},2}(T) = Q_{\mathrm{st}} \tag{12}$$

Putting Eq. (12) into Eqs. (10) results in:

$$\begin{aligned} U_{1\mathrm{d}} &= U_{\mathrm{r}} + \frac{Q_{\mathrm{i},1}(T_{\mathrm{o}})}{C} - \frac{Q_{\mathrm{st}}}{C} \\ U_{2\mathrm{d}}(T) &= U_{\mathrm{r}} + \frac{Q_{\mathrm{i},2}(T)}{C} - \frac{Q_{\mathrm{st}}}{C} \end{aligned} \tag{13}$$

Let us characterize ER by $\Delta U(T)$, a deviation of the plateau voltage level of premature AP from the reference AP:

$$\Delta U(T) = U_{2\mathrm{d}}(T) - U_{1\mathrm{d}} \tag{14}$$

Putting Eqs. (13) into Eq. (14) and extending to the term $Q_{\mathrm{i},1}(T)/C$ results in:

$$\begin{aligned} \Delta U(T) &= \frac{Q_{\mathrm{i},1}(T) - Q_{\mathrm{i},1}(T_{\mathrm{o}})}{C} - \frac{Q_{\mathrm{i},1}(T) - Q_{\mathrm{i},2}(T)}{C} \\ &= \frac{\Delta Q^{\mathrm{p}}(T)}{C} - \frac{\Delta Q^{\mathrm{s}}(T)}{C} \end{aligned} \tag{15}$$

where:

$$\begin{aligned} \Delta Q^{\mathrm{p}}(T) &= Q_{\mathrm{i},1}(T) - Q_{\mathrm{i},1}(T_{\mathrm{o}}) = \sum_{j=1}^{n} [Q_{\mathrm{i},1,j}(T) - Q_{\mathrm{i},1,j}(T_{\mathrm{o}})] \\ \Delta Q^{\mathrm{s}}(T) &= Q_{\mathrm{i},1}(T) - Q_{\mathrm{i},2}(T) = \sum_{j=1}^{n} [Q_{\mathrm{i},1,j}(T) - Q_{\mathrm{i},2,j}(T)] \end{aligned} \tag{16}$$

Properties and measurements of the parameters ΔQ^{p} and ΔQ^{s}

The term $\Delta Q^{\mathrm{p}}(T)/C$, which is related exclusively to the reference test AP1, reflects the effects of variable initial conditions and hence the restitution processes proper. The total value of the charge $\Delta Q^{\mathrm{p}}(T)$ can be experimentally obtained by imposing the stored regular steady-state AP1 after abbreviated interval T (Fig. 2), as follows from Eqs. (15), (16), (11), and (12):

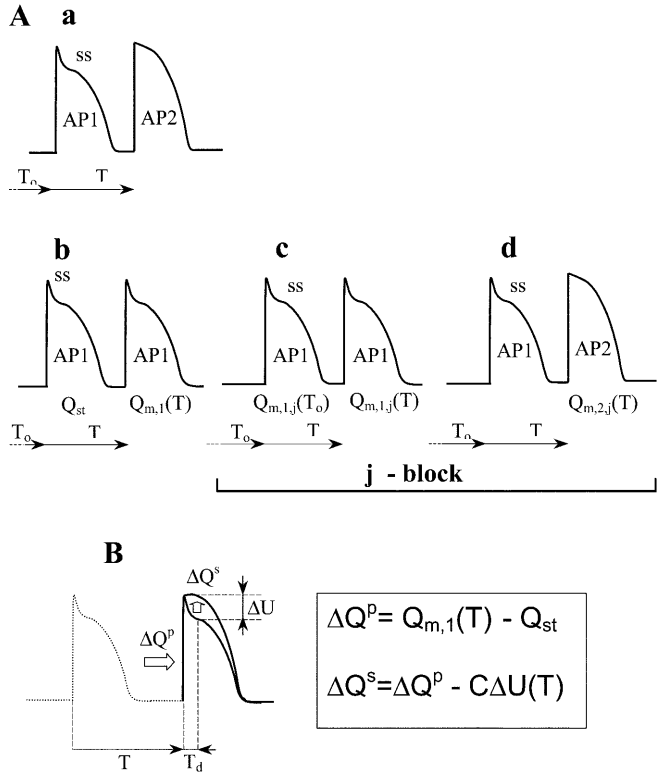

Fig. 2 **A** Experimental protocols used for determining the electrical restitution and its components in terms of charge parameters. **a** The configuration of natural steady-state (*ss*) and premature APs are stored for subsequent use as control voltage-clamp pulses AP1 and AP2, respectively. T_o, basal interval; T, test interval. **b** ΔQ^p is determined from the response to AP1 (control steady-state configuration) applied as both steady-state and premature pulses. **c** *j*-th component of ΔQ^p is determined by protocol **b**, but after pharmacological blockade of the examined membrane current. **d** *j*-th component of ΔQ^s is determined from the response to control clamp configuration AP1-AP2 (**a**) after the blockade of the examined membrane current. *Below* are the obtained charges necessary for the calculation of the components according to Eqs. (19) and (20). **B** Calculation of the total ER courses described by ΔQ^p and ΔQ^s; C, membrane capacity; Q_{st}, charge of the stimulation impulse used to trigger the AP

$$\begin{aligned}\Delta Q^p(T) &= Q_{i,1}(T) - Q_{i,1}(T_o)\\ &= Q_{m,1}(T) - Q_{m,1}(T_o) = Q_{m,1}(T) - Q_{st}\end{aligned} \tag{17}$$

The term $\Delta Q^s(T)/C$ reflects the effect of the variability of the test pulses AP2 under the same initial conditions (secondary processes).

It follows that Eq. (15) describes the primary and secondary restitution processes separately, thus satisfying the first condition stated above.

By virtue of Eqs. (16), the ER curves take the form of the sum of the contributions of individual current components represented by charges transferred by ionic currents across the membrane during interval T_d. Thus, the "charge representation" also complies with the second condition.

The individual components of ionic current contributing to parameters ΔQ^p and ΔQ^s as defined in Eqs. (15) and (16) are experimentally separable with specific blocking agents. Let us denote by $Q_{m,1,j}(T)$ and $Q_{m,2,j}(T)$ the charges supplied from the external source in response to voltage-clamped action potentials AP1 and AP2 after blocking the *j*-th current component. Equations (10) apply both before and after the exposure of the cell to any drug. Consequently:

$$\begin{aligned}Q_{i,1,j}(T) &= Q_{m,1}(T) - Q_{m,1,j}(T),\\ Q_{i,2,j}(T) &= Q_{m,2}(T) - Q_{m,2,j}(T)\end{aligned} \tag{18}$$

Putting Eqs. (18) into Eqs. (16) under the consideration of Eq. (12) results in:

$$\begin{aligned}\Delta Q^p(T) &= \sum_{j=1}^{n}\left[Q_{i,1,j}(T) - Q_{i,1,j}(T_o)\right]\\ &= \sum_{j=1}^{n}\left[Q_{m,1}(T) - Q_{m,1,j}(T) + Q_{m,1,j}(T_o) - Q_{st}\right]\end{aligned} \tag{19}$$

$$\begin{aligned}\Delta Q^s(T) &= \sum_{j=1}^{n}\left[Q_{i,1,j}(T) - Q_{i,2,j}(T)\right]\\ &= \sum_{j=1}^{n}\left[Q_{m,1}(T) - Q_{m,1,j}(T) + Q_{m,2,j}(T) - Q_{st}\right]\end{aligned} \tag{20}$$

Only those components of $\Delta Q^p(T)$ which correspond to the currents primarily affected by variable initial conditions are different from zero. The share of component *j* on the ER described by ΔQ^p may be estimated by the triple application of reference standard AP1 which has been stored under control conditions (Fig. 2A, a). First, after abbreviated test interval T at control conditions; second and third, after premature (T) and regular (T_o) intervals under the drug effect (b and c in Fig. 2A). The charges may be obtained by the integration of the recorded currents. The contributions of individual components may also be ascertained by the additive application of the respective blocking agents (as illustrated in Results). $\Delta Q^s(T)$ can be dissociated into its components in a similar way. In this case, however, both premature and regular APs must be stored for clamping under the effect of the drugs (Fig. 2A, d). Since ΔQ^p and ΔQ^s are expressed by Eqs. (19) and (20) as sums of measurable components, the above third condition is also met.

ER tested by imposed pulses different from the AP

ER itself is sufficiently defined by ΔQ^p. In order to specify $\Delta Q^p(T)$ and its components, it is unnecessary to choose the recommended form of the conditioning and test pulses, i.e. the natural course of the steady-state AP stored in the computer memory. The rectangular (or other) clamp pulses, approximating the voltage and duration of the AP at the given frequency and temperature, can offer satisfactory results of analysis comparable to those obtained with AP clamp pulses (see Fig. 13c, below).

If the test pulse differs from AP, the simplifying condition of Eq. (12) is not applicable and instead of Eq. (19) the separation of the j-th component of total charge restitution has to be performed using the more general form:

$$\Delta Q^{\mathrm{p}}(T) = Q_{\mathrm{i}}(T) - Q_{\mathrm{i}}(T_{\mathrm{o}}) = Q_{\mathrm{m}}(T) - Q_{\mathrm{m}}(T_{\mathrm{o}}) = \sum_{j=1}^{n} \left[Q_{\mathrm{m}}(T) - Q_{\mathrm{m},j}(T) + Q_{\mathrm{m},j}(T_{\mathrm{o}}) - Q_{\mathrm{m}}(T_{\mathrm{o}}) \right] \tag{21}$$

Introducing the notation:

$$Q_j^{\mathrm{p}}(T) = Q_{\mathrm{m}}(T) - Q_{\mathrm{m},j}(T),\ \Delta Q_j^{\mathrm{p}}(T) = Q_j^{\mathrm{p}}(T) - Q_j^{\mathrm{p}}(T\mathrm{o}) \tag{22}$$

we finally obtain:

$$\begin{aligned} Q_{\mathrm{m}}(T) &= \sum_{j=1}^{n} Q_j^{\mathrm{p}}(T), \\ \Delta Q^{\mathrm{p}}(T) &= \sum_{j=1}^{n} \Delta Q_j^{\mathrm{p}}(T) \end{aligned} \tag{23}$$

An example of the experimental protocol used to assess the charges necessary for calculating the components of $\Delta Q^{\mathrm{p}}(T)$ is illustrated in Fig. 3.

Results

ER represented by parameters of AP

The ER curves were first reconstructed from two customary parameters characterizing the time course of premature APs (Fig. 4): the membrane voltage achieved at 100 ms after the onset of the stimulating pulse (APV_{100}), or the time to 50% repolarization (APD_{50}). At the given frequency (0.5 Hz) and temperature (30 °C), both parameters constantly exhibited an early overshoot, peaking at 0.4 s on average. The overshoot exceeded the steady-state values (i.e. at 2 s intervals) by about 10%.

First, we tried to assess the role of the individual current components of the AP restitution overshoot with their selective blockade. However, it became evident that the ER tested by APs was determined not only by the recovery processes which took place during the rest period, but that it was also contaminated by the processes occurring during the variable test AP until the moment of parameter reading. We termed the former events as primary and the latter, also comprising time-independent current components, as secondary.

This perplexity is illustrated in Fig. 5. It shows the steady-state APs and the ensuing premature APs (at test intervals of 300 ms) recorded at control conditions and after the application of two selective blocking agents: 4-aminopyridine (4-AP) and verapamil. It is obvious that owing to the dramatic effects of the drugs, all current components contributing to the configuration of the premature test APs must have changed substantially. This also holds true for the time-independent currents, which by definition do not undergo restitution. Thus, identification and quantification of the current components underlying the primary restitution events require experimental protocols consisting of uniform voltage-clamped pulses instead of free-running APs. In this case,

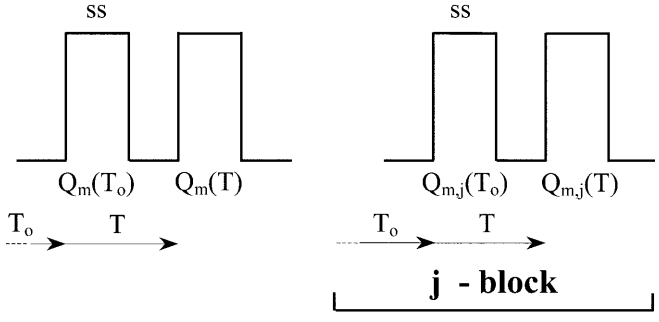

Fig. 3 Experimental protocols composed of rectangular pulses for determining the primary components of charge-ER. T_{o}, basal interval; T, test interval. *Below* are the obtained charges necessary for calculation according to Eq. (21). $\Delta Q^{\mathrm{p}}(T)$ is determined from the response to the steady state and the premature test pulse (*left*). The j-th component of $\Delta Q^{\mathrm{p}}(T)$ is determined by applying the same protocol after the pharmacological blockade of the examined membrane current

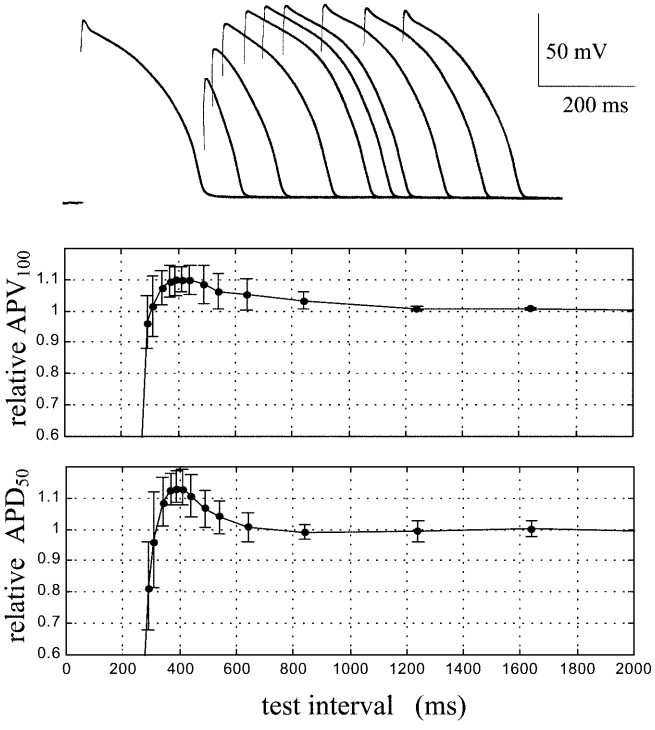

Fig. 4 Electrical restitution represented by AP parameters. *Upper panel*: original records of constant steady-state AP and the APs following variable test (coupling) intervals. *Middle and lower panels*: ER curve represented, respectively, by membrane voltage 100 ms after the onset of the stimulation impulse (APV_{100}) and AP duration at 50% level of repolarization (APD_{50}). The mean values of six experiments ± SEM, normalized to a basal stimulation rate of 0.5 Hz. Dog trabeculae; temperature 30 °C

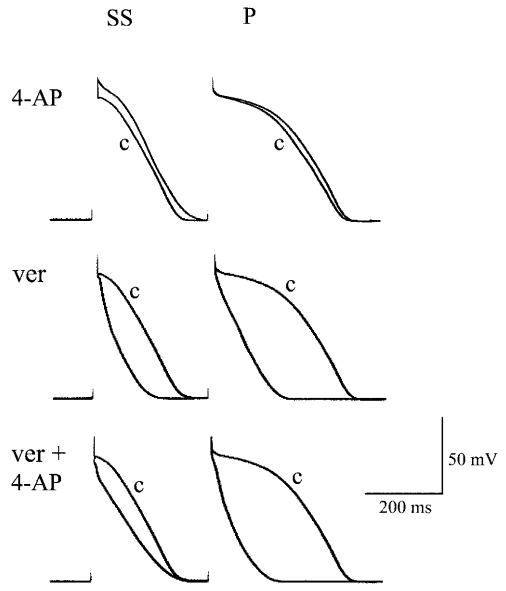

Fig. 5 Original records from a representative experiment of the steady state (*SS*) and premature (*P*) AP before (*c*) and after the administration of 2 mM 4-aminopyridine, 10 μM verapamil, and both drugs together. Dog ventricular trabecula; basal rate 0.5 Hz; coupling interval 300 ms

a selective block of one current component leaves the voltage-dependent gating of the others unaffected.

ER represented by instantaneous values of ionic currents

To obtain a principal idea about ER-determining ionic currents, the last control and the successive premature test APs were substituted by rectangular voltage-clamp pulses (300 ms duration to plateau level) approximately imitating the AP configuration (Fig. 6). The ER curve conspicuously matched the recovery of the slow inward current (I_{si}) that had been earlier identified with the calcium inward current (I_{Ca}). However, as revealed by later research, I_{si}, conventionally measured as the difference between the peak inward current and the level attained after 300 ms, is quite complex. It may be strongly affected by a current component carried by electrogenic Na/Ca exchange (I_{NaCa}) and particularly by two components of the transient outward current I_{to}: the voltage-controlled 4-AP-sensitive current (I_{to1}) and the current activated by actual intracellular Ca^{2+} (I_{to2}).

We restricted our analysis to the dissociation of total ionic current response (after the elimination of the initial brief I_{Na}) into the following components (Fig. 7): the verapamil-sensitive component I_{vs}, the 4-AP-sensitive component I_{to1}, the delayed outward current I_K, and the time-independent background current I_{bg}. In dog ventricular cells, the transient outward current cannot be assessed from the total current trace at control conditions since it is masked by the prevailing I_{Ca} (Fig. 7, trace a). This is fully revealed by the I_{vs} block (Fig. 7, trace b). However, verapamil does not inhibit only I_{Ca}. The secondary decay of $[Ca^{2+}]_i$ also affects the other Ca-dependent currents: I_{NaCa} and I_{to2}. In this representative experiment, 4-AP abolished I_{to1} (trace c). The time course of I_{to1} and I_{vs} (presumably composed of I_{Ca}, I_{to2}, and I_{NaCa}) may be reconstructed as the differences b–c and a–b, respectively. The residual current is then easily dissociable into the time-dependent I_K and time-independent I_{bg}.

In spite of the striking similarity between the ER curves represented by APD_{50} and I_{si} (Fig. 6), even the instantaneous values of currents measured in response to uniform test pulses cannot be regarded as adequate parameters for quantitative characterization of APD or APV restitution. It is the velocity of change (time derivative) of the membrane voltage at a given instant that is determined by the total ionic current (see Dis-

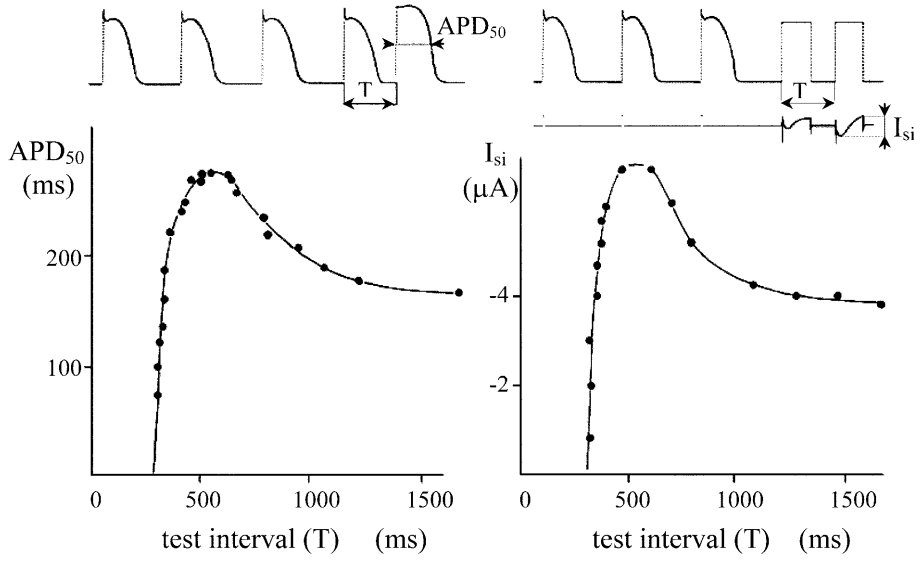

Fig. 6 The comparison of the ER curve expressed in terms of APD_{50} (*left*) and of slow inward current recovery (*right*). The *upper panels* illustrate the experimental protocols and parameters measured. *T*, test interval

cussion, Eq. 24), while both AP-derived parameters are determined by the previous time course of the ionic current.

ER represented by transferred charges

Primary events

As indicated in Theory, the electric charge transferred by the ionic current across the membrane in response to a uniform depolarizing impulse is the proper parameter, which can yield reasonable estimates of the share of current components on the variations of APV (and, as a rule, also on APD) during ER. Figure 7 illustrates the charges as areas delimited by current traces in control and under the effects of drugs (left panel), and the results of the dissociation of the total charge into its components (right panel). The above arithmetic applies to both currents and the respective charges. For the sake of easy comparison with the usual ER curves, the charges are defined and plotted with reversed signs (see Eqs. 7 and 9).

Figure 8 presents a charge-interval plot from another representative experiment (the sequence of blocking agents is reversed with respect to Fig. 7). Electric charges were obtained in the described procedure as integrals of the total recorded current. Because of the inaccurate measurement of I_{Na} under the given experimental conditions, this current was eliminated by starting the integration with a 10 ms delay. The missing I_{Na} and consequently Q_{Na} shifted all the curves in Fig. 8 to more negative values, which remained constant for all intervals beyond 380 ms. In the case of shorter intervals, the slope of the early rising phase of ER is slightly underestimated owing to the incomplete recovery of I_{Na} from inactivation.

The initial steady state was achieved by a train of clamp pulses (300 ms, 80 mV) at 0.5 Hz. The regular and test pulses were identical. The evaluation of the total charge was performed under control conditions (Fig. 8a), after blocking I_{to1} (Fig. 8b), and eventually after the additional suppression of I_{Ca} and Ca^{2+}-sensitive currents (Fig. 8c). The straight line (Fig. 8d) represents the charge Q^{p}_{bg} transferred by the time-independent component I_{bg}. The charge-ER curve shows an overshoot under control conditions, its depression after I_{to1} inhibition (with reference to the end-point), and complete abolition under the simultaneous inhibition of I_{to1} and I_{vs}. In line with the analysis shown in Fig. 7 and Eqs. (21), (22), and (23), curves a, b, and c in Fig. 8 respectively represent charges $Q_m(T) - Q^{p}_{Na} = Q^{p}_{to1} + Q^{p}_{vs} + Q^{p}_{K} + Q^{p}_{bg}$ (Eq. 23), $Q_{m,4-AP}(T) - Q^{p}_{Na} = Q^{p}_{vs} + Q^{p}_{K} + Q^{p}_{bg}$, and $Q_{m,4-AP+vs}(T) - Q^{p}_{Na} = Q^{p}_{K} + Q^{p}_{bg}$ (Eq. 22).

As line d in Fig. 8 corresponds to charge Q^{p}_{bg}, the differences a–b, b–c, and c–d enable direct resolution of the charge-ER curve, as measured under control con-

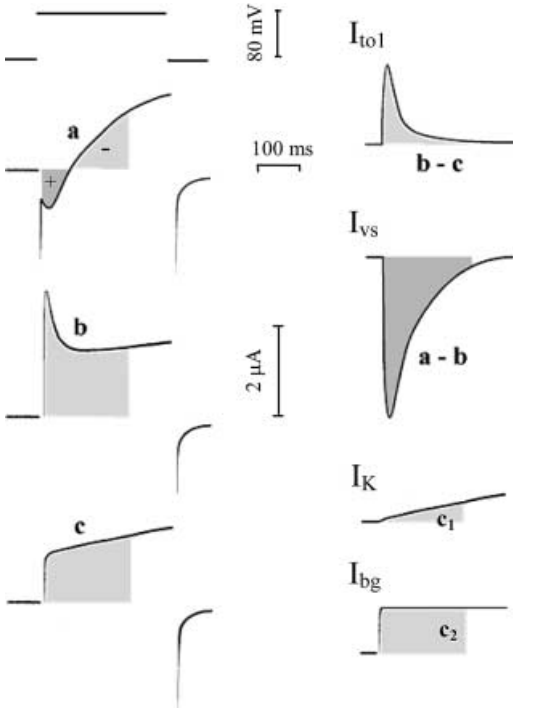

Fig. 7 Dissociation of the total ionic current into its major components in voltage-clamped dog trabecula. Current responses to 300 ms, 80 mV pulses from holding voltage = resting voltage in normal Tyrode solution (*a*), under the effect of verapamil (*b*), and verapamil + 4-AP (*c*). I_{to1} was reconstructed as *b–c*; I_{vs} as *a–b*. I_{bg} and I_K were evaluated from *c* as the initial step and the time-dependent increase of current, respectively. The recorded currents were integrated between 10 and 200 ms from the onset of depolarization. The integrals corresponding to the charges transferred by the respective current components are shown by *shaded areas*. Note their sign in accord with their definition (Eqs. 7)

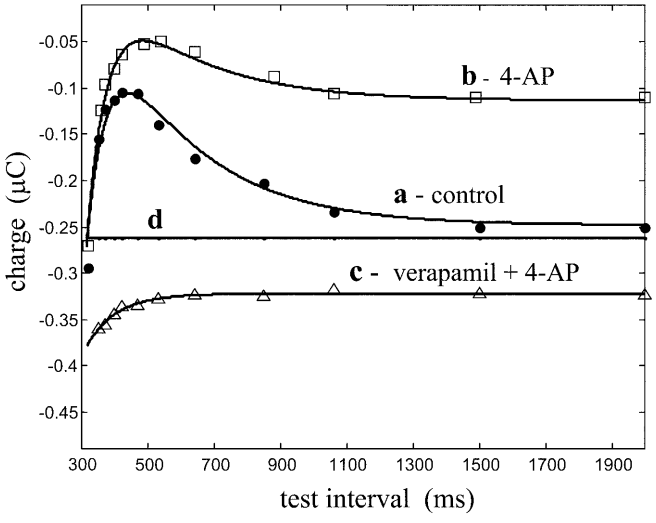

Fig. 8 ER curves represented by transferred charges during depolarization clamp pulses (80 mV from the resting level). Plotted are the charges obtained by the integration of ionic membrane currents in the interval 10–200 ms from the onset of the pulse. *a* Charge-ER curve at control conditions; *b* after 2 mM 4-AP; and *c* under the combined effect of 4-AP and 10 µM verapamil. *d* The charge carried by the time-independent current component

ditions (Fig. 8, curve a), into its respective components Q^{p}_{to1}, Q^{p}_{vs}, Q^{p}_{K}, and Q^{p}_{bg}. Their development during restitution is shown in Fig. 9. Curve Q^{p}_{vs}, comprising verapamil-sensitive current components, is biphasic with an overshoot. Curve Q^{p}_{to1} characterizes the recovery from inactivation of current I_{to1}. Charge Q^{p}_{K}, which is transferred by the delayed outward current, is augmented at the shortest test intervals, since its channels are still activated. During ER, the absolute value of Q^{p}_{K} exponentially declines with a time constant corresponding to I_K deactivation.

The term $\Delta Q^{p}(T)$, constructed in accord with Eqs. (21), (22), and (23), makes it possible to assess the role of individual current components in making up the ER curve. ΔQ^{p} and its components (Fig. 10) are the deviations of the transferred charges from their steady-state values. The arrows indicate the values of the charge components at the test interval of maximum overshoot (450 ms). ΔQ^{p}_{to1} is responsible for 50% of the overshoot. The rest is accounted for by the modulation of the $[Ca^{2+}]_i$-sensitive current components ΔQ^{p}_{vs}. The deviation of the test charge ΔQ^{p}_{K} from that at a steady state has a tendency to suppress the overshoot. In the given example its share is rather small. It counteracts the overshoot-generating currents by about 6%.

Resolution of primary and secondary events

The next objective was to separate the ER curve modulation due to the events which take place exclusively prior to the test pulse (primary factors, net restitution) from those generated by the variation of the test pulse (secondary factors). The measure of the former is the difference between the charges tested by a standardized pulse (stored steady-state AP) inserted after an abbreviated test interval and after a regular test interval (ΔQ^{p}). The measure of the latter is the difference between the charges tested by standardized and free-running APs of identical prematurity (ΔQ^{s}).

The above analysis was performed on a quantitative model defined by a system of non-linear differential equations. Essentially it is a version of a system proposed by Nordin (1993), modified in that it is supplemented by a quantitative description of I_{to1}. The model is specified in Methods. In contrast to biological experiments, the computer simulations yield the time courses of all the components of membrane ionic current under both voltage- and current-clamp regimens, therefore representing an ideal tool for the verification of theoretical deductions.

Figure 11 illustrates the primary and secondary components of the charge-ER curve plotted in voltage units (charge over membrane capacity) in the middle panel. Their time course reveals an overshoot similar to their difference (lower panel), which characterizes the ER curve by APV_{50} (ΔU). However, the quantities $\Delta Q^{p}/C$ and $\Delta Q^{s}/C$ are approximately 14 times larger than ΔU. This fact is in agreement with the hypothesis that the incomplete recovery of some current components may affect the ensuing AP configuration in a negative feedback manner (in the given example, feedback with 14-fold amplification). The nature of this feedback control is the voltage dependence of the plateau-determining currents.

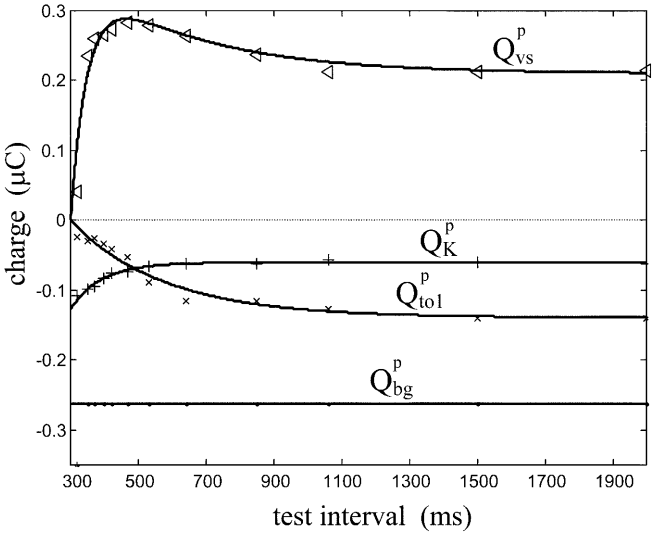

Fig. 9 Dissociation of charge restitution (*a* in Fig. 8) into components: 4-AP-sensitive Q^{p}_{to1}, verapamil-sensitive Q^{p}_{vs}, delayed rectifier Q^{p}_{K}, and background Q^{p}_{bg}. The dissociation was carried out from the differences of charge-ER curves from Fig. 8: Q^{p}_{to1} as *a–b*, Q^{p}_{vs} as *b–c*, Q^{p}_{K} as *c–d*, and Q^{p}_{bg} as *d*

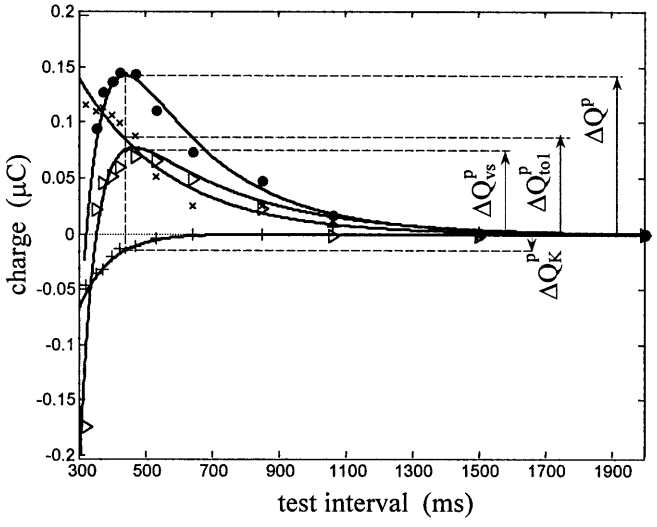

Fig. 10 The quantitative evaluation of the contribution to the charge-ER curve (ΔQ^{p}) of the individual components shown in Fig. 9. Plotted are the charges transferred by time-dependent current components versus the test interval T after the subtraction of the respective steady state values (at $T = T_o$), i.e. curves from Fig. 9 shifted to a common end-point. ΔQ^{p} is the charge-ER curve (the shifted curve *a* from Fig. 8); and ΔQ^{p}_{vs}, ΔQ^{p}_{to1}, and ΔQ^{p}_{K} are the components of ΔQ^{p}. The values were measured at the peak of ΔQ^{p}

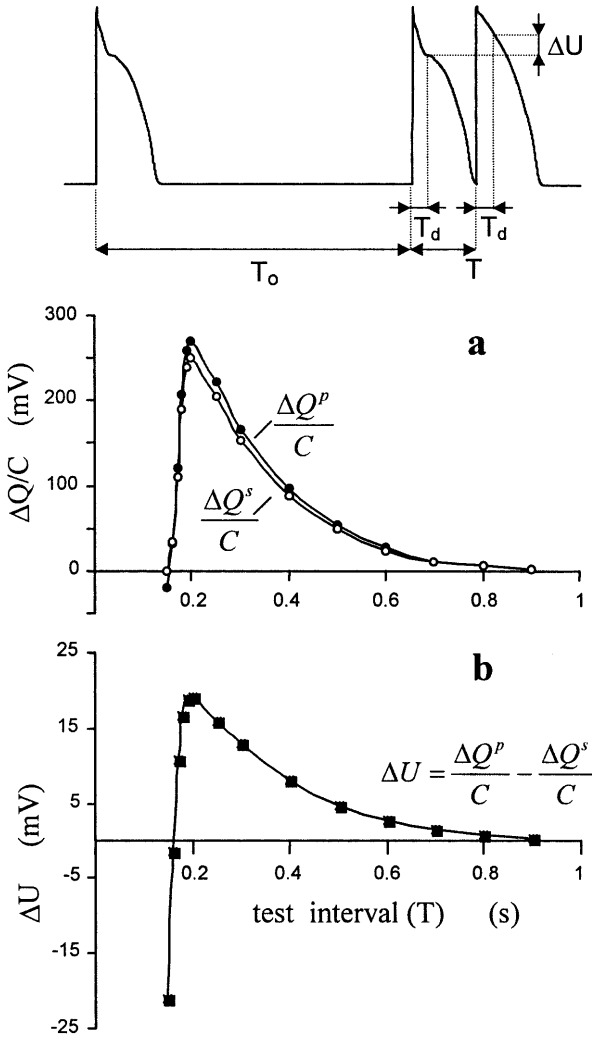

Fig. 11a, b Charge restitution curves obtained by computer simulations. The *upper panel* illustrates the course of two successive calculated steady-state APs ($T_o = 1$ s) and of a premature AP ($T = 0.2$ s). **a** The ER curves of primary (ΔQ^p) and secondary (ΔQ^s) processes calculated at $T_d = 50$ ms. The charges were divided by membrane capacity and thus recalculated to voltage units. **b** The difference between both curves shown in **a** gives the ER curve represented by ΔU (a deviation of APV_{50} from the steady-state value)

Figure 12 shows the individual contributions of charge-represented ionic currents to $\Delta Q^p(T)$ and $\Delta Q^s(T)$. The charges were obtained on the basis of computer simulations using Eqs. (16). Simulations based on Eqs. (19) and (20) were also done to verify the formulae proposed for the experimental analysis. The main primary components in the given model (components of ΔQ^p) are ΔQ^p_{to1}, ΔQ^p_{Ca}, and ΔQ^p_{NaCa}. The principal components which tend to compensate for the primary changes (components of ΔQ^s) are ΔQ^s_{Ca} and ΔQ^s_{NaCa}. The other components, including ΔQ^s_K, play little role.

The results of the dissociation of ΔQ^p and ΔQ^s is demonstrated in Fig. 13 for the test interval T of the maximum overshoot of the ER curve. Provided that the sum of the absolute values of all components of ΔQ^p (or ΔQ^s) is considered to be 100%, then in the tested model 60% of the primary augmentation of AP is accounted for by I_{to1}, 25% by I_{Ca}, and 5.6% by I_{to2}. I_{NaCa} and I_K suppress the overshoot by 7.6% and 2%, respectively (Fig. 13a). The resulting elevated plateau generates secondary, counteracting changes of currents, predominantly I_{Ca} and I_{NaCa} with respective shares of 78% and 12.5% (Fig. 13b). The secondary events include the time-independent (and hence missing among the primary events) I_{bg}. However, its share in ΔQ^s is rather small owing to the relatively short period of integration of $T_d = 50$ ms.

To quantify the influence of the reference impulse on the assessment of the primary current components, we alternately used either a rectangular pulse mode (Fig. 13c) or an AP mode, applying the waveform recorded at maximum restitution overshoot (Fig. 13d). These simulations gave an estimate of the spread of values obtained with various test impulses. With an appropriate magnitude of the rectangular test pulse, virtually identical results may be obtained, as with natural AP clamping. The employment of rectangular impulses as described in the previous section is thus justified.

Discussion

Action potential- and current-derived parameters

Each cardiac membrane excitation is followed by processes of gradual recovery which determine the generation and configuration of the forthcoming AP. These processes are summarily denoted as electrical restitution (Bass 1975), in analogy to mechanical restitution, i.e. the recovery of contractility during the interbeat interval (Bravený and Kruta 1958).

The mechanisms underlying ER have been widely studied experimentally in multicellular preparations (Iinuma and Kato 1979; Šimurda and Šimurdová 1991; Kobayashi et al. 1992; Qi et al. 1997; Szigligeti et al. 1998) and in the single cardiomyocytes (Hiraoka and Kawano 1987; Tseng 1988; Szigligeti et al. 1998) of various species, including humans (Nanasi et al. 1996; Bányász et al. 1997); owing to obvious implications, they have also been studied clinically (Franz et al. 1988; Endresen and Amlie 1989; Morgan et al. 1992b). Recently, the clinical aspects of ER have been analysed by means of mathematical models as well (Kogan et al. 1997; Qu et al. 1999). In addition to the significant tissue and species differences of ER, striking ischemic alterations have been ascertained (Dilly and Lab 1988; Kurz et al. 1994; Taggart et al. 1996). In these studies, the most frequently used quantitative parameters of ER have been the membrane voltage attained at a given time after the onset of AP (APV) and the duration of AP at a given level of repolarization (APD).

It has been found that the ER curve represents a monotonic, sometimes biphasic, or even more complex

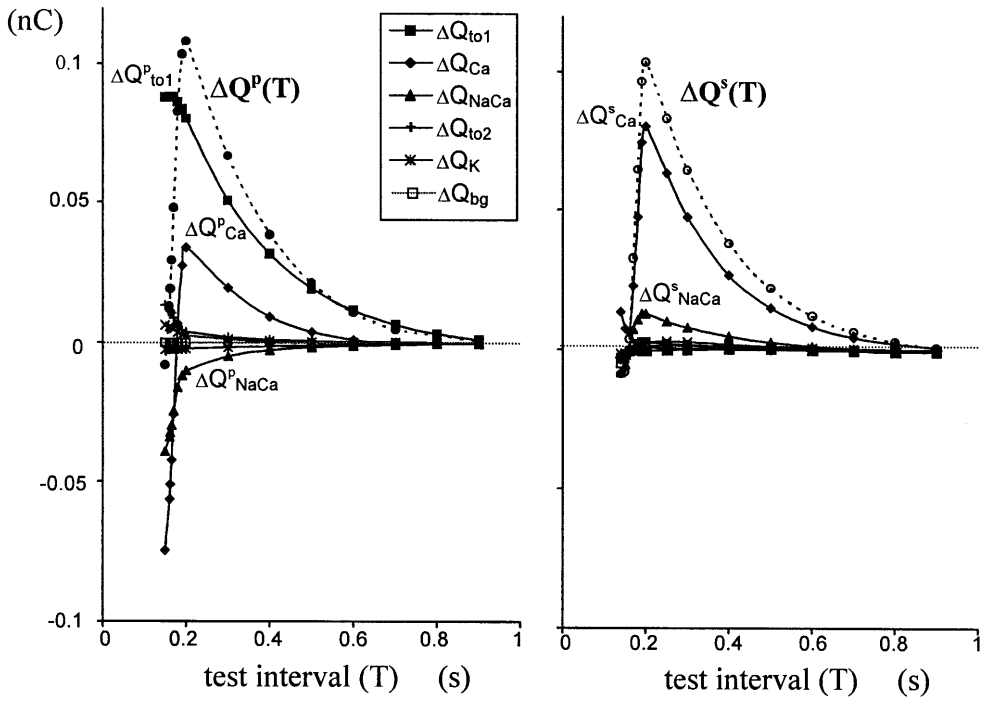

Fig. 12 Dissociation of ΔQ^{p} and ΔQ^{s} (*dashed lines*) into their constituents corresponding to individual currents (*full lines*). The components that contribute to the total by less than 2% were omitted

function of the stimulus coupling interval. In a frequently observed biphasic form, APD and APV transiently increase to a maximum (overshoot) and then gradually decrease to a steady-state value with further prolongation of the premature interval. The various courses of ER can be explained by the species or tissue differences, including the heterogeneity within the ventricular wall (Litovsky and Antzelevitch 1989; for review see Antzelevitch et al. 1991). Different experimental conditions may also play a role, e.g. temperature (Bjornstad et al. 1993), basal cycle length (Boyett and Jewell 1978; Elharrar and Surawitz 1983), and stretching (Horner et al. 1994). The accumulation and depletion of ions in narrow intercellular clefts necessarily affect ionic currents and consequently ER. The same characteristic species differences of ER were however observed both in multicellular preparations and in isolated myocytes (Szigligeti et al. 1998). Based on a study of canine ventricular cells, Robinson et al. (1987) concluded that the restitution processes underlying APD are not markedly dependent on the presence or absence of restricted extracellular spaces.

The individual current components responsible for the ER course have been evaluated from AP parameters or directly from voltage-clamp experiments utilizing pharmacological interventions that suppress individual AP-generating ionic currents. It is generally assumed that the shape of the ER curve, particularly the occurrence of the overshoot (supernormal AP), depends on the interplay of species-specific time constants of the recovery of characteristic current components. For example, it has been suggested that the deactivation of two components of I_K (I_{Kr} and I_{Ks}) plays a primary role in the initial fast phase of the ER curve in guinea pig ventricular cells (Zeng et al. 1995). On the contrary, the recovery from inactivation of L-type I_{Ca} seems to be the decisive factor in dogs (Šimurda and Šimurdová 1991) and in humans (Bányász et al. 1997). The later course of ER is apparently affected mainly by I_{to}, I_{NaCa}, I_K, and I_{Ca} in association with the recoveries of voltage-gated systems and of ionic concentrations (particularly $[Ca^{2+}]_i$ and $[K^+]_e$). The substantial role of these components has been proved recently by Janvier et al. (1997) in a detailed study (combined current-clamp and voltage-clamp experiments) in ferret ventricular cells. These authors emphasize that the evaluation of the current components from the differences between APD restitution curves before and after pharmacological intervention is only approximate. The reason is that the altered course of the test AP simultaneously changes the time course of all currents involved in the AP configuration. To our knowledge, a quantitative analysis of ER with regard to these components has so far not been performed.

Electric charge: the due parameter

The advantage of evaluating electrical restitution by APD or APV is that it demonstrates the result of restitution by an uncomplicated, generally understandable parameter. However, the analysis of ER based on pharmacologically induced variations of AP can hardly provide unambiguous conclusions concerning the underlying ionic current components. The elimination of any current component significantly alters the AP configuration and hence the course of other voltage-dependent components.

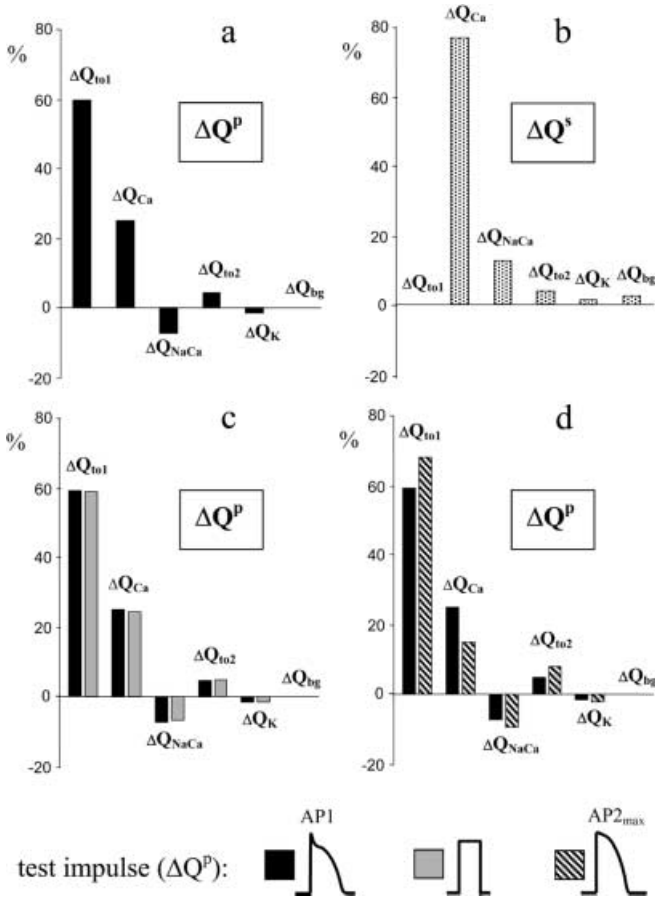

Fig. 13a–d Relative contributions of the main components to the charge-ER curve at maximum overshoot (see Fig. 12). **a** Components of $\Delta Q^{p}(T)$ tested by the imposed steady-state AP (AP1: primary events). **b** Components of $\Delta Q^{s}(T)$ tested by the imposed steady state, and premature APs (AP1, AP2: secondary events). **c**, **d** Comparison of the data of **a** (*full columns*) with the data obtained by rectangular pulses to +15.4 mV (**c**, *shaded columns*), and by maximum, supernormal AP (**d**, *hatched columns*)

The records of membrane currents obtained in response to uniform clamp pulses are near the authentic restitution process, provided the protocol approximates the natural holding and action potentials. The initial conditions of the pharmacologically unaffected components, as well as the secondary events during the uniform test pulse, remain constant. The question is how to quantitatively evaluate the contribution of individual current components to ER and at the same time to observe APD and APV as the commonly used parameters.

According to Eq. (4) in Theory (considering that $I_m = 0$ when the stimulus is over), the magnitude of the ionic current at a given time of AP corresponds to the velocity of change of the membrane voltage:

$$I_i = \sum_{j=1}^{n} I_{i,j} = -C\frac{dU}{dt} \qquad (24)$$

but not to the usual parameters, voltage U (i.e. APV) or the time of repolarization (i.e. APD). However, the same equation implies that the charge transferred by I_i is linearly related to U. The variation of APV in the course of ER is directly proportional to the sum of electric charges related to individual ionic current components [Eqs. (15) and (16)]. While $\Delta Q^{s}(T)$ represents the secondary events caused by the changes of the test pulse, the term $\Delta Q^{p}(T)$ (i.e. the difference in charge transferred by ionic currents across the membrane during premature and regular pulses of equal size) meets the criteria for a parameter of net (primary) restitution. It is the sum of individual current contributions, which can be separated according to Eq. (19) (generally Eq. 21) and quantitatively defined during the whole course of ER (see Figs. 10, 11, 12, 13).

The computer simulations show that the primary and secondary terms in Eq. (15) differ from each other only slightly, although their charge components are clearly dissimilar (Fig. 12). In Fig. 11a they are expressed in voltage units as $\Delta Q^{p}(T)/C$ and $\Delta Q^{s}(T)/C$. They follow a time course similar to their difference ΔU that is, however, much smaller (Fig. 11b). This conclusion is supported by the experimental results. In all six experiments presented in Fig. 4, the maximum overshoot of APV_{100} (expressed in voltage units) was constantly reproducible, but at least six times less than the overshoot on the charge restitution curve (see ΔQ^{p} in Fig. 10), recalculated to voltage units as $\Delta Q^{p}/C$.

If the first term, ΔQ^{p}, in Eq. (15) defines the initial conditions, then the features of the second term, ΔQ^{s}, may be interpreted as strong negative feedback which equilibrates the positive and negative current components and minimizes the possible excessive change of AP configuration. In other words, owing to their voltage dependence, the primary changes of these components induce secondary changes, which keep the total ionic current low enough to prevent large deviations of plateau voltage. In this sense, the resulting change of plateau level ΔU may be considered a deviation of the controlled quantity.

Of course, it is not the only feedback mechanism controlling AP configuration. For instance, excessive diversity of APD is prevented by the feedback control of I_K (Surawicz 1992). It is possible to speculate that the early after-depolarizations reflect an instability of these highly non-linear feedback systems.

Limitations of the analysis

A prerequisite of the described analysis is the possibility to block the single components of ionic current without interference with other components. It is assumed that a uniform steady state and test pulses will secure constant conditions for all currents except the blocked one. However, some interventions may alter the ionic concentrations, namely $[Ca^{2+}]_i$ and $[K^{+}]_e$, thereby indirectly modifying the unblocked calcium- or potassium-sensitive currents. This was the reason why we did not attempt to further resolve the verapamil-sensitive current I_{vs}.

Other complicating factors are the limited specificity and the use-dependency of most blocking agents (Hondeghem and Katzung 1984). Owing to these factors, the blockade of membrane channels need not be complete in the whole range of test intervals.

The time integrals of gating currents (charge movements) appear to be negligible in comparison with the integrals of the respective ionic currents, though the peak values of the currents may be comparable. The reason is the short duration of the gating currents. For example, the records from guinea pig ventricular myocytes (Hadley and Lederer 1991) give an estimate of bound charge movement of less than 2% of the of charge transferred by L-type I_{Ca}.

As the analysis is based on voltage-clamp measurements, the possible error due to the cable properties depends on the accuracy of the voltage-clamp measurement. The voltage-clamp method itself requires a fairly small size of preparation (or their tested parts) with respect to the space constant for the effect of the cable properties to be negligible.

The accumulation and depletion of ions in intercellular clefts does not represent any limitation of the method above either. It is aimed at establishing the contribution of current components to the changes of AP configuration irrespective of their mechanism. Naturally, the quantitative assessment of the role of ion concentrations in ER formation would be significantly upgraded through comparison of the data (in terms of electrical charges) obtained in a multicellular preparation and in an isolated myocyte of the same animal.

The form of the test pulse does not affect the identification of the current components that constitute the primary restitution process. Their relative share is retained with reasonable accuracy (Fig. 13c, d).

Supernormal premature action potential

As mentioned above, the overshoot of restitution is obviously due to several current components of different magnitude and kinetics. Their relative contributions depend on too many factors and generally valid conclusions are impossible to draw.

The described approach to the analysis of ER was applied to our experimental data from canine ventricular muscles (verification on isolated guinea pig and rat myocytes using the AP clamp technique will be the subject of our next study). We demonstrated in all experiments that the overshoot observed in AP parameters (APV_{100}, APD_{50}) was also present on the charge-ER curve. Its analysis (Fig. 10) indicates that the overshoot is primarily due to 4-AP-sensitive I_{to1} and verapamil-sensitive I_{vs}. The latter may comprise not only I_{Ca} but also the current of the electrogenic Na/Ca system I_{NaCa}, the $[Ca^{2+}]_i$-dependent transient outward current I_{to2}, and possibly other minor components modulated by $[Ca^{2+}]_i$. On the other hand, the overshoot is partly diminished by I_K.

Analogous results were obtained with a modified computer model, which had originally been developed for guinea pig cardiomyocytes (Nordin 1993). However, the prerequisite of the appearance of a marked overshoot was the introduction of I_{to1}. The overshoot was augmented by I_{Ca} and slightly by I_{to2}. On the other hand, it was diminished by I_{NaCa}, which is directly related to intracellular Ca^{2+} release and represents an inward-going current parallel to mechanical restitution (Šimurda et al. 1992). Therefore, it enhances APV, prolongs APD, and levels off the restitution in its later course.

Action potential- and charge-restitution

Resolution (Eq. 15) into primary and secondary charge components holds exactly for the expression of ER by means of APV. The question is whether it is applicable also in the analysis of ER described by APD. As a rule, the courses of ER curves described by APD and APV differ (see Fig. 4). APV is usually read during the early plateau phase (time T_d), i.e. well before the time of reading the commonly used APD_{50} or APD_{90}. These differences may be minimized if APV_{Td} is measured after a longer interval T_d corresponding to control APD (e.g. APD_{50}). The relation between ER curves constructed in these two modes can be described in terms of the differences between the measured and the reference (steady state) values of APD and APV (ΔAPD and ΔAPV):

$$\Delta\,\mathrm{APD} = CI_{i,mean}\Delta\,\mathrm{APV} \tag{25}$$

where $I_{i,mean}$ is the mean value of the ionic current in the interval between the steady state and the actual value of APD. If $I_{i,mean}$ remains constant during ER, the normalized ΔAPD and ΔAPV restitution curves are identical. This condition (disputable in the presence of large I_K) can be best evaluated from AP time derivatives during restitution. In this respect, the computer simulations based on APD_{50} produced the same courses of normalized ΔAPD and ΔAPV restitution curves.

In conclusion, the present approach to the analysis of ER makes it possible to separate the two modes of its current components: those which actually describe the proper recovery events and those which are secondarily modified by inherent variations of the test action potential.

In contrast to the methods employed so far (which offer qualitative or semiquantitative, i.e. rather approximate, data), the present method is rigorously quantitative. The ER curve is expressed as a sum of the contributions of individual current components represented as the charge.

Although the charge-ER curves were derived from the voltage-restitution curves, they correspond reasonably well with the curves constructed from the time dimension of the action potential.

Acknowledgements This study was supported by a grant from the Grant Agency of the Czech Republic (GA ČR-305/97/0043) and grant CEZ:J07/98:141100004 from the Czech Ministry of Education.

References

Antzelevitch C, Sicouri S, Litovsky SH, Lukas A, Krishnan SC, Di Diego JM, Gintant GA, Liu D-W (1991) Heterogeneity within the ventricular wall. Electrophysiology and pharmacology of epicardial, endocardial, and M cells. Circ Res 69:1427–1449

Bányász T, Magyar J, Szigligeti P, Pankucsi C, Varró A, Nánási PP (1997) Frequency-dependent characteristics of human cardiac muscle. Exp Clin Cardiol 2:205–209

Bass BG (1975) Restitution of the action potential in cat papillary muscle. Am J Physiol 228:1717–1724

Bjornstad H, Tande PM, Lathrop DA, Refsum H (1993) Effects of temperature on cycle length dependent changes and restitution of action potential duration in guinea pig ventricular muscle. Cardiovasc Res 27:946–950

Boyett MR, Jewell BR (1978) A study of the factors responsible for rate-dependent shortening of the action potential in mammalian ventricular muscle. J Physiol (Lond) 285:359–380

Bravený P, Kruta V (1958) Dissociation de deux facteurs: restitution et potentiation dans l'action de l'intervalle sur l'amplitude de la contraction du myocarde. Arch Int Physiol Biochim 66:633–652

Dilly SG, Lab MJ (1988) Electrophysiological alternans and restitution during acute regional ischaemia in myocardium of anaesthetised pig. J Physiol (Lond) 402:315–333

Elharrar V, Surawicz B (1983) Cycle length effect on restitution of action potential duration in dog cardiac fibres. Am J Physiol 244:H782–H789

Endresen K, Amlie JP (1989) Electrical restitution and conduction intervals of ventricular premature beats in man: influence of heart rate. Pacing Clin Electrophysiol 12:1347–1354

Franz MR, Swerdlow CD, Liem LB, Schaefer J (1988) Cycle length dependence of human action potential duration in vivo. Effects of single extrastimuli, sudden sustained rate acceleration and deceleration, and different steady-state frequencies. J Clin Invest 82:972–979

Hadley RW, Lederer WJ (1991) Ca^{2+} and voltage inactivate Ca^{2+} channels in guinea-pig ventricular myocytes through independent mechanisms. J Physiol (Lond) 444:257–268

Hiraoka M, Kawano S (1987) Mechanism of increased amplitude and duration of the plateau with sudden shortening of diastolic intervals in rabbit ventricular cells. Circ Res 60:14–26

Hondeghem LM, Katzung BG (1984) Antiarrhythmic agents: the modulated receptor mechanism of action of sodium and calcium channel-blocking drugs. Annu Rev Pharmacol Toxicol 24:387–423

Horner SM, Dick DJ, Murphy CF, Lab MJ (1994) Cycle length dependence of the electrophysiological effects of increased load on the myocardium. Circulation 94:1131–1136

Iinuma H, Kato K (1979) Mechanism of augmented premature responses in canine ventricular muscle. Circ Res 44:624–629

Janse MJ, Wit AL (1989) Electrophysiological mechanisms of ventricular arrhythmias resulting from myocardial ischemia and infarction. Physiol Rev 69:1049–1169

Janvier NC, McMorn SO, Harrison SM, Taggart P, Boyett MR (1997) The role of Na^{+}-Ca^{2+} exchange current in electrical restitution in ferret ventricular cells. J Physiol (Lond) 504:301–314

Kawano S, Hiraoka M (1991) Transient outward currents and action potential alterations in rabbit ventricular myocytes. J Mol Cell Cardiol 23:681–693

Kobayashi Y, Peters W, Khan SS, Mandel WJ, Karaguezian HS (1992) Cellular mechanisms of differential action potential duration restitution in canine ventricular muscle cells during single versus double premature stimuli. Circulation 86:955–967

Kogan BY, Karplus WJ, Karpoukhin MG, Roizen IM, Chudin E, Qu Z (1997) Action potential duration restitution and electrical excitation propagation in a ring of cardiac cells. Comput Biomed Res 30:349–359

Koller ML, Riccio ML, Gilmour RF Jr (1998) Dynamic restitution of action potential duration during electrical alternans and ventricular fibrillation. Am J Physiol 275:H1635–H1642

Kurz RW, Ren XL, Franz MR (1994) Dispersion and delay of electrical restitution in the globally ischaemic heart. Eur Heart J 15:547–554

Litovsky SH, Antzelevitch Ch (1989) Rate dependence of action potential duration and refractoriness in canine ventricular endocardium differs from that of epicardium: role of the transient outward current. J Am Clin Cardiol 14:1053–1066

Morgan JM, Cunningham D, Rowland E (1992a) Dispersion of monophasic action potential duration: demonstrable in humans after premature ventricular extrastimulation but not in steady state. J Am Clin Cardiol 19:1244–1253

Morgan JM, Cunningham D, Rowland E (1992b) Electrical restitution in the endocardium of the intact human right ventricle. Br Heart J 67:42–46

Nanasi PP, Varro A, Pankucsi C, Homolay P, Knilans TK, Kovacs L, Papp GJ, Lathrop DA (1996) Electrical restitution in diseased human ventricular myocardium. Clin Physiol 16:339–351

Nordin C (1993) Computer model of membrane current and intracellular Ca^{2+} flux in the isolated guinea pig ventricular myocyte. Am J Physiol 265:H2117–H2136

Peineau N, Garnier D, Argibay JA (1992) Rate dependence of action potential duration and calcium current in isolated guinea-pig cardiocytes. Exp Physiol 77:615–625

Qi A, Tang C, Yeung-Lai-Wah JA, Kerr CR (1997) Characteristics of restitution of rabbit atrium. Can J Physiol Pharmacol 75:255–262

Qu Z, Weiss JN, Garfinkel A (1999) Cardiac electrical restitution properties and stability of reentrant spiral waves: a simulation study. Am J Physiol 276: H269–H283

Robinson RB, Boyden PA, Hoffman BF, Hewett KW (1987) Electrical restitution process in dispersed canine cardiac Purkyne and ventricular cells. Am J Physiol 253:H1018–H1025

Šimurda J, Šimurdová M (1991) Electrical restitution in canine ventricular muscle. Scr Med 64:67–80

Šimurda J, Šimurdová M, Bravený P, Šumbera J (1976) Slow inward current and action potentials of papillary muscles under non-steady state conditions. Pflügers Arch 362:209–218

Šimurda J, Šimurdová M, Čupera P (1988) 4-Aminopyridine sensitive transient outward current in dog ventricular fibres. Pflügers Arch 411:442–449

Šimurda J, Šimurdová M, Bravený P, Šumbera J (1992) A contraction-related component of slow inward current in dog ventricular muscle and its relation to Na^{+}-Ca^{2+} exchange. J Physiol (Lond) 456:49–70

Surawicz B (1992) Role of potassium channels in cycle length dependent regulation of action potential duration in mammalian cardiac Purkynje and ventricular muscle fibres. Cardiovasc Res 26:1021–1029

Szigligeti P, Bányász T, Magyar J, Szigeti G, Papp Z, Varro A, Nánási PP (1998) Intracellular calcium and electrical restitution in mammalian cardiac cells. Acta Physiol Scand 163:139–147

Taggart P, Sutton PM, Boyett MR, Lab M, Swanton H (1996) Human ventricular action potential duration during short and long cycles. Rapid modulation by ischemia. Circulation 94:2526–2534

Tseng G-N (1988) Calcium current restitution in mammalian ventricular myocytes is modulated by intracellular calcium. Circ Res 63:468–482

Tseng G-N, Hoffman BF (1989) Two components of transient outward current in canine ventricular myocytes. Circ Res 64:633–647

Watanabe M, Otani NF, Gilmour RF (1995) Biphasic restitution of action potential duration and complex dynamics in ventricular myocardium. Circ Res 76:915–921

Wu TJ, Yashima M, Doshi R, Kim YH, Athill CA, Ong JJ, Czer L, Trento A, Blanche C, Kass RM, Garfinkel A, Weiss JN,

Fishbein MC, Karagueuzian HS, Chen PS (1999) Relation between cellular repolarization characteristics and critical mass for human ventricular fibrillation. J Cardiovasc Electrophysiol 10:1077–1086

Yanagisawa T, Taira N (1979) Positive inotropic effect of 4-aminopyridine on dog ventricular muscle. Naunyn-Schmiedeberg's Arch Pharmacol 307:207–212

Zeng J, Laurita KR, Rosenbaum DS, Rudy Y (1995) Two components of delayed rectifier K^+ current in ventricular myocytes of the guinea pig type: theoretical formulation and their role in repolarization. Circ Res 77:140–152